D.L. Wood and T.J. Wipf

Heavy Agricultural Loads on Pavements and Bridges

Sponsored by the
Iowa Department of Transportation and the
Iowa Highway Research Board

March 1999

Iowa DOT Project HR-1073

Iowa Department of Transportation

report

FINAL

College of Engineering
Iowa State University

D.L. Wood and T.J. Wipf

Heavy Agricultural Loads on Pavements and Bridges

Sponsored by the Iowa Department of Transportation
and the Iowa Highway Research Board

March 1999

Iowa DOT Project HR-1073

engineering research institute
iowa state university

ABSTRACT

During the harvest season in Iowa, it is common to have single axle loads on secondary roads and bridges that are excessive (typical examples are grain carts) and well beyond normal load limits. Even though these excessive loads occur only during a short time of the year, they may do significant damage to pavements and bridges. In addition, the safety of some bridges may be compromised because of the excessive loads, and sometimes there may be little indication to the users that damage may be imminent. At this time there are no Iowa laws regulating axle loads allowed for agricultural equipment. This study looks at the potential problems this may cause on secondary roads and timber stringer bridges.

Both highway pavement and timber bridges are evaluated in this report. A section (panel) of Iowa PCC paved county road was chosen to study the effects of heavy agricultural loads on pavements. Instrumentation was applied to the panel and a heavily loaded grain cart was rolled across. The collected data were analyzed for any indication of excessive stresses of the concrete.

The second study, concerning excessive loads on timber stringer bridges, was conducted in the laboratory. Four bridge sections were constructed and tested. Two of the sections contained five stringers and two sections had three stringers. Timber for the bridges came from a dismantled bridge, and deck panels were cut from new stock. All timber was treated with creosote. A hydraulic load was applied at the deck mid-span using a foot print representing a tire from a typical grain cart. Force was applied until failure of the system resulted. The collected data were evaluated to provide indications of load distribution and for comparison with expected wheel loads for a typical heavily loaded single axle grain cart.

Results of the pavement tests showed that the potential of over-stressing the pavement is a possibility. Even though most of the tension stress levels recorded were below the rupture strength of the concrete, there were a few instances were the indicated tension stress level exceeded the concrete rupture strength. Results of the bridge tests showed that when the static ultimate load capacity of the timber stringer bridge sections was reached, there was sudden loss of capacity. Prior to reaching this ultimate capacity, the load sharing between the stringers was very uniform. The failure was characterized by loss of flexural capacity of the stringers. In all tests, the ultimate test load exceeded the wheel load that would be applied by an 875 bushel single axle grain cart.

TABLE OF CONTENTS

LIST OF FIGURES

LIST OF TABLES

INTRODUCTION

During the harvest season in Iowa, it is common to have single axle loads on secondary roads and bridges that are excessive (typical examples are grain carts) and well beyond normal load limits. Even though these excessive loads occur only during a short time of the year, they can do significant damage to pavements and bridges. In addition, the safety of some bridges may be compromised because of the excessive loads, and sometimes there may be little indication to the users that damage may be imminent.

OBJECTIVE

The objective of the work described in this report was to perform experimental tests on a Portland Cement Concrete (PCC) pavement panel in the field, and perform experimental tests on a representative section of a timber stringer bridge in the laboratory to assess the structural performance under severe loads. The tests were performed with loads intended to simulate extreme loading conditions. Data were collected and are presented in this report. The testing was also documented using video tape and photographs.

SCOPE

To meet the objectives above, a PCC pavement section of County Road V71 was chosen by the Iowa Department of Transportation for heavy axle load testing. Loading was applied using a loaded grain cart slowly crossing over the test pavement panel using a tractor. This was repeated numerous times, with strain data being collected during each run. Induced stresses in the pavement were evaluated from these data.

The objectives above were further met for the timber stringer bridges by testing four typical stringer bridge sections to ultimate capacity. Two of the bridges had five stringer cross sections and two had three stringer cross sections. The collected data provided ultimate load behavior and also provided insight into the lateral load distribution of the system.

PAVEMENT TESTS

PCC Test Panel Description

County Road V71 in Buchanan County, Iowa was chosen by the Iowa Department of Transportation for this series of tests (Figure 1). This road was constructed in the early to mid 1960's. The test panel was a nominal 11 ft (3.35 m) wide and 36 ft (10.97 m) long. The thickness was 6 in. (152.4 mm) across the entire panel. Before testing, the panel was visually mapped for cracks and no major cracks were observed. Only minor hairline cracks, similar to shrinkage cracks, were visible along with a small, 36 sq. in. (23,226 sq. mm) asphalt patch in the northwest corner of the test panel. Figure 2 shows the location of this patch. This location was determined to be far enough away from the strain gage locations so that it would have minimal effect on the results. The pavement panels immediately adjacent to the test panel did show some significant cracking. Concrete cores were removed from the pavement by the Iowa Department of Transportation and tested to determine the concrete strength.

Instrumentation and Location

The pavement strains were measured by strain gages mounted on the panel top surface at locations to obtain maximum levels due to grain cart wheel loads (see Figure 2). Five gages, Hitec Products model HBP-35-2000-C-3VR, were bonded to the concrete using preparation techniques recommended by the Measurements Group, Inc. Tech Tip TT-611. The gages had a gage length of 2 in. and were encapsulated in a protective coating. The adhesive used was M-Bond AE-10, also manufactured by the Measurements Group, Inc. An elevated temperature of 125°F (51.7°C) was applied to the gage simultaneously with a pressure of 10 psi (68.9 kPa) for two hours (Figure 3) while the adhesive cured. After curing was complete, the gages and wires were taped down to the concrete and protected from possible damage and attached to the data acquisition system. Data was collected using an Optim Megadac 5108DC which was controlled by a laptop PC. A scan rate of 50 samples per second was used based on the crawl velocity of approximately 5 mi/h (8 km/h), the speed at which the grain cart test vehicle was to be passed over the test panel.

The gage locations were determined using procedures outlined in Ref.[1]. Assumptions made included a modulus of elasticity, E, equal to 4.5 x 10^6 psi (31 Gpa), a modulus of subgrade reaction, k, equal to 100 pci (27.1 N/cm^3) and a Poisson ratio, μ, of 0.18. Since the final test loads had not been determined prior to the test, two more assumptions were made for determining gage locations; an assumed wheel load, P, of 20,000 lbs. (88.96 kN) and an assumed loaded tire pressure, p, ranging from a minimum of 45 psi to 100 psi maximum (310 to 689 kPa). Substitution into Equation 1 gave the radius of relative stiffness, l, as being equal to 30.25 in. (768.4 mm). Using Equation 2 to determine a, the radius of the tire footprint, the distance, a_l,

$$l = \left(\frac{Eh^3}{12(1-\mu^2)k} \right)^{0.25} \qquad \text{Eq. 1}$$

$$a = \sqrt{\frac{P}{p\pi}} \qquad \text{Eq. 2}$$

which is the distance to the point of action of the load on a common angle bisection at the slab corner, is equal to $\sqrt{2}a$. Therefore, the assumed value for locating the gages fell between 30.0 and 38.0 in. (762.0 and 965.2 mm). The final wheel load for the grain cart test vehicle was actually 18,500 lbs. (82.29 kN) and loaded tire pressure was measured at 45 psi (310 kPa). This resulted in an actual a_l dimension of 37.2 inches (944.9 cm). The actual positions of Gages 1 through 5 were 31.00, 31.00, 35.00, 38.00 and 37.00 in. (787.4, 787.4, 889.0, 965.2, and 939.8 mm), respectively (Figure 2). These values were chosen in order to provide a range that would include areas of maximum stress. Gages 4 and 5 were positioned closest to the maximum computed stress level. The final layout of the gages is shown in Figure 2.

Test Procedure

The grain cart was attached to a tractor and pulled toward the south across the test panel with the cart outside wheel positioned near the edge of the slab (see Figure 4). After the cart was pulled in that direction and data was collected, the test was repeated with the tractor pushing the

cart toward the north taking care to try to use the same wheel path. A total of 28 passes was made (15 from north to south and 13 from south to north) on the panel.

Test Results

Concrete Core Tests

From the average of three concrete core compression tests performed by the Iowa Department of Transportation, the concrete strength was determined to be 7,677 psi (53 Mpa). Using this concrete strength and Equation 3, the estimated modulus of rupture was found to equal 657 psi (4,530 kPa).

$$f_r = 7.5\sqrt{f_c'} \qquad \text{Eq. 3}$$

Load Tests

Due to a configuration error in the data acquisition system, data from Gage 1 was not accurate and was not included in this report.

All of the tests performed indicated similar behavior of the pavement panel. Figure 5 shows a typical strain vs. time plot for one of the tests. There was little difference in the pavement behavior when the cart was pulled either north to south, or pushed south to north. The average maximum reading for Gage 2 was 25 micro-strains in tension and -39 micro-strains in compression. Gage 3 had maximum and minimum averages of 16 micro-strains in tension and -8 micro-strains in compression. Gage 4 average values were 24 micro-strains in tension and -44 micro-strains in compression. Gage 5 average maximum values were 64 micro-strains in tension and -6 micro-strains in compression. Table 1 tabulates these maximum and minimum values along with means and medians for all of the tests. Four of the tests resulted in some higher than normal tension values for Gage 5. The median value for all of the tests on Gage 5 was 44.5 micro-strains in tension. Gage 5 values in tension for, Tests 1, 3, 16, and 27 were 200, 125, 131, and 258 micro-strains. Test 1 plotted data are shown in Figure 6. Similar behavior was recorded in Tests 3, 16 and 27. Maximum stress values were calculated as 900, 562.5, 589.5, and 1,161 psi (6205, 3,878, 4,064, and 8,004 kPa). In general, the stress values in Gage 5 were in the range of 200 psi (1,379 kPa), with the other gage positions showing maximum ranges of 120 psi (827 kPa).

Evaluation of Test Results

Calculated tensile stresses for Tests 1 and 27 were 900 and 1,161 psi (6,205 and 8,004 kPa), respectively, at the Gage 5 location, which exceeded the modulus of rupture of 657 psi noted above by 37% and 77%, respectively. As stated earlier, the five gage locations were determined prior to knowing all of the test variables, and it should be noted that the Gage 5 location was the closest of all of the gages to the position determined from the actual weight and tire pressure of the grain cart to be the highest strain location. As illustrated in Table 1, the median values for Gage 5 were the highest of all the gages.

Although there were two tests where Gage 5 values were high, the lack of repeatability and infrequent occurrence of these magnitudes could be a result of one of the following observations. Visual observation noted that the exact path of the grain cart tire was not the same on every pass. This may not only cause the observed scatter in strain levels, but there were occasions when the tires from the tractor rolled over the gage, which might result in localized inaccurate readings from that gage. The tractor and grain cart tires also rolled over the wiring that connected the gage to the data acquisition system on occasion, which potentially could also cause a false reading. After the 28 tests were performed, there were no noticeable additional cracks in the pavement surface. Video recording of the joint location between adjacent panels showed significant relative deflections occurring between adjacent panels.

Summary and Conclusions

Generally, the loads used in these tests did not appear to cause over stressing of the pavement surface at the gaged locations. However, an occasional high recorded strain indicates that a potential problem may exist. A more controlled test series monitoring exact load paths, improved sensor position, and modification of the sensor connection detail would allow for a more accurate interpretation of the results. The grain cart loads used in this study did not represent worse-case loading situations. An increased load could accentuate any problems to a greater extent. Other factors that may further affect stress levels include temperature and moisture content of the subsoil.

TIMBER STRINGER BRIDGE TESTS

Timber Bridge Description

Four ultimate load tests were performed on timber stringer bridges in the Structural Engineering Laboratory in the Town Engineering Building on the Iowa State University campus. Nominal 4-in. x 12-in. stringers were used from an existing bridge. The nominal 3-in. x 12-in. planks, sill plates, headers, and blocking were cut from new timber. All timber was treated with creosote. The stringers were toenailed into the sill plate with four 60d x 6-in. ring nails spaced 16 in. (406.4 mm) on centers. The sill plate was bolted to concrete supports, and positioned to allow for a 16 ft (4.88 m) span. The planks were nailed perpendicular to the stringers with three nails at each stringer.

Test Procedure and Instrumentation

The load was applied at midspan of the bridge using a 50-ton (445 kN) hydraulic ram. The ram applied the load through a 30-in. x 20-in. footprint (simulating a tire or wheel for a grain cart trailer) designed to distribute the force uniformly in the center of the bridge deck. Between the metal footprint and bridge planks were six 10-in. x 10-in. x 1-in. neoprene pads arranged to provide the required loading area. The 30-in. (762 mm) dimension was parallel to the bridge span. A 50 kip (222 kN) electronic load cell was used to monitor the applied load. Deflections were recorded at the mid-span of each stringer, and at some chosen support locations using Celesco string potentiometer transducers with a resolution of 0.001 in. (0.025 mm) Photographs and video tapes of the tests were taken. Data was collected using a PC controlled Optim Megadac system. The system is the same as used in the pavement tests. The scan rate was set at one scan of every channel per second through failure.

Test Results and Evaluation

Bridge 1

The bridge was built to the dimensions as shown in Figure 7. The finished bridge is shown in Figure 8. Deflections were recorded at the mid-span of each stringer, and at the support

of the middle stringer at each end. The accompanying data plot, Figure 9, shows the five mid-span stringer deflections versus the load.

The overall failure mode of the bridge was due to flexural failure of the stringers. Note that, up to 24,000 lbs., the slope on the load/deflection plot was linear for all the stringers. The slope was the smallest for the middle stringer (3M) during this period of loading. This indicates that it was carrying a larger portion of the total applied load in comparison to the other stringers, assuming that all five stringers had the same stiffness. Based on the same stiffness assumption, the outside two stringers (1N and 5S) carried the smallest portion of the load, as exhibited by the steepest load/deflection slope. From 24,000 to 36,000 lbs. (106.7 to 160.1 kN), note that the slope of the middle stringer decreased significantly from the earlier loading up to 24,000 lbs. (106.7 kN), becoming nonlinear. The other four stringers continued to exhibit essentially the same load/deflection behavior from 24,000 to 36,000 lbs. (106.7 to 160.1 kN), as exhibited in the load range up to 24,000 lbs. (106.7 kN). These results indicate that the load sharing of the middle stringer was essentially the same, but a reduction in the stiffness occurred, possibly due to substantial cracking in the beam. At 36,000 lbs. (160.1 kN), the load dropped 2,000 lbs. (8.9 kN), and the load/deflection behavior (resembling a saw tooth) was similar for each stringer. When the changes in deflection of each stringer due to this drop in the load are compared, the greatest change occurred in the middle stringer. This behavior was most likely caused by the significant opening of cracks (splits) in the middle stringer and an instantaneous loss of resistance by the stringer. Therefore, the data collection rate was not fast enough to capture this event. From 36,000 lbs. (160.1 kN) until the ultimate capacity of the bridge at 42,200 lbs. (106.7 kN), the load/deflection slopes of each stringer decreased slightly from the previous load range. When the ultimate capacity of 42,200 lbs. (187.7 kN) was reached, the load/deflection behavior became erratic, making it difficult to obtain meaningful behavioral information from these data. Only several data points were recorded after the ultimate load was reached for the stringers, and one string potentiometer disengaged from a stringer due to the failure, thus providing little useful data. The short load/deflection plateau evident at this failure load represents a redistribution of the load to the stringers that had not failed yet after the initial failure of a stringer. It is also characterized

by the significant opening of the cracks in the failed stringers. Once this load redistribution occurred, the subsequent bridge failure was sudden.

Figures 10 through 13 show splits that took place in some stringers resulting in the failure of the bridge. Note that stringers 1N, 2IN, 3M, and 4IS all exhibited major splits at failure. From the data plot, it appears that stringer 3M failed first and the splitting was most likely initiated by a flaw in the bottom tension fibers near mid-span. Stringer 1N failed next, followed closely by stringers 2IN and 4IS. A visual inspection of the sill plates showed no noticeable crushing of the wood under the stringers. Inspection of the deck planks also indicated that there was no noticeable damage. Failure of the bridge was sudden and was characterized by flexural failure of the stringers.

Bridge 2

The measured dimensions and completed bridge are shown in Figures 14 and 15. Due to an error in the data collection storing process, no load/deflection plot was obtained for this test. However, during the test, a continuous real time load/deflection plot was observed on the DAS computer monitor, and these data were used in the discussion of results. In addition, the following discussion was based on notes taken during the test, visual observation, and review of photographs and video tape.

Based only on the observation data mentioned above, it was noted that the first major crack occurred in stringer 4IS at a load of 28,000 lbs. (124.6 kN). Up to that load it was observed that the load/deflection plot was linear with the pairs of symmetrically loaded stringers behaving as in the Bridge 1 test. The two interior stringers (2IN and 4IS) had slightly less load/deflection slopes, indicating they were carrying a larger load compared with the outside stringers. The middle stringer (3M) deflected the most, indicating that it was carrying most of the load. From about 3,000 lbs. to 10,000 lbs. (13.3 to 44.5 kN), typical sounds described as popping and cracking due to the straining of the bridge and bridge stringers occurred. At 18,800 lbs. (83.6 kN), the sounds became more pronounced and distinct, indicating that significant cracking or fiber straining was beginning to occur. At this point, it was observed on the DAS monitor that stringer 4IS was deflecting more than stringer 2IN. At 28,000 lbs. (124.6 kN), a significant crack occurred in stringer 4IS. It appeared that the crack was initiated at a knot in the tension face of the stringer

(Figure 16). From 28,000 lbs. to 35,000 lbs. (124.6 to 155.7 kN), it was observed visually that the crack in stringer 4IS continued to open wider and additional cracking sounds, or fiber straining, could be heard coming from other stringers. At 39,000 lbs. (173.5 kN), the applied load dropped to 35,000 lbs. (155.7 kN) due to a failure in stringer 5S. It was also noticed that string 3M, the middle stringer, had developed a crack. It is believed that this crack occurred after stringer 4IS failed and before the failure of stringer 5S. Again, this crack seems to have been initiated by a knot in the wood close to the stringer tension face (see Figure 17). Additional loading back up to 39,000 lbs. (173.5 kN) resulted in horizontal cracking in stringer 5S (see Figure 18). The real time plot observed on the DAS monitor for the test at this point showed that the stringer mid-span deflections ranged from the smallest in stringer 1N to the largest in stringer 5S. This suggests that the final failure would occur in stringers 4IS or 5S. The ultimate load for the bridge was 40,100 lbs. (178.4 kN). Stringer 5S incurred considerable flexural cracking (see Figure 18). Stringers 1N and 2IN did not show any signs of distress or damage. The deck planks did not show any load distress. Failure of the bridge was sudden and characterized by the flexural failure of the stringers.

Bridge 3

This bridge was built using three stringers instead of five as used in Bridges 1 and 2. However, the construction details were similar to Bridges 1 and 2. The deck planks were a nominal 3-in. by 12-in. and were kept at a length of 6 ft (1.8 m) as for Bridges 1 and 2, since it was determined that the additional overhang would not affect the test results. Figure 19 shows the measured dimensions and Figure 20 shows the constructed bridge prior to testing. The same loading apparatus was used as in Bridges 1 and 2, and the instrumentation was similar with the following changes. Deflections were recorded at the east support on stringers 1N and 2M. Mid-span deflections were recorded on all three stringers and at the support on the west ends of stringers 2M and 3S.

Noteworthy visual observations prior to testing included some splintering from weathering at the tension face (bottom) of stringer 1S at mid-span. In addition, the middle stringer (2M) had a minor split at the east support that appeared to run the full length of the stringer at about mid-depth. There also appeared to be some warping or twisting of stringer 2M at the west end.

Figure 21 shows the load/deflection plot for the test. At a load of 3,000 to 5,000 lbs. (13.3 to 22.2 kN) noticeable bridge and/or fiber straining noises occurred. At 18,000 lbs. (80.1 kN), sounds of cracking could be heard and small clouds of dust could be seen coming off the bottom of the stringers. Referring to the plot, it appears as if stringer 2M, which contained the horizontal split, deflected less than stringer 3S but more than stringer 1N. At 23,000 lbs. (102.3 kN), the bottom of stringer 2M split significantly, resulting in a drop in the load of 1,000 lbs. (4.4 kN), and the deflection became greater than that of stringer 3S. Further loading resulted in an ultimate load of 27,200 lbs. (121 kN). At this point, stringer 3S suddenly failed near mid-span. Visual observation indicated that the failure initiated at a knot. A large piece at the east end of stringer 3S broke off and fell to the floor (see Figure 22). The split in the bottom of stringer 2M opened up considerably. There was no major damage noted to stringer 1N (see Figure 23). From the plot it appears that stringer 2M failed first and the sudden additional load to stringer 3S caused its failure. This may be supported by the fact that the load/deflection plots of these two stringers cross on Figure 21. The overall result of the bridge failure can be seen in Figure 24. Inspection of the deck planks indicated that there was no noticeable damage. Failure of the bridge was sudden and characterized by flexural failure of the stringers.

Bridge 4

Bridge 4 was constructed similarly to Bridge 3. Figure 25 shows the measured dimensions. The only change from Bridge 3 was that the deck planks were offset to the south side so that the north end had a deck overhang of 6 in.(152.4 mm). This offset left an overhang of approximately 28 in. (711.2 mm) on the south side of the bridge. This was done primarily so that the photographs and video would more clearly document visually the outside stringer (1N) behavior. Instrumentation and loading were also similar to Bridge 3. Figure 26 shows the bridge prior to testing.

Visual observations prior to testing noted a knot in the tension face (bottom) of stringer 1N near mid-span, some minor surface splitting of stringer 3S near mid-span, and significant weathering at the inside face of stringer 1N.

The load/deflection plot for this test is shown in Figure 27. At a load of 5,000 lbs. (22.2 kN), noticeable bridge and/or fiber straining noises occurred. From the beginning of the

bridge response, stringer 1N exhibited stiffer load/deflection behavior than stringers 2M and 3S (this statement is based on all three stringers carrying an equal percentage of the applied load). At about 17,000 lbs. (75.6 kN), the slope/deflection plot of stringer 1N increased, indicating that there was an increase in the load distribution to stringers 2M and 3S. At 27,000 lbs. (120.1 kN), the slopes of the load/deflection plot became nonlinear. At 34,000 lbs. (151.2 kN), it was observed visually that a crack formed in stringer 3S. The ultimate load was 36,300 lbs. (161.5 kN) with stringer 3S developing a major flexural crack and some major horizontal cracking (see Figure 28). Some cracking also occurred in stringer 2M at mid-span. Inspection of stringer 1N showed that some noticeable cracking was beginning to develop near the knot in the tension fibers, evident by the splitting of the wood around the knot. The final condition of Bridge 4 after the failure is seen in Figure 29. None of the deck planks were damaged. Failure of the bridge was sudden and was characterized by flexural failure of the stringers.

Significance of Test Results

It is of interest to compare the experimental test results with expected performance in a field bridge. To do this, a comparison is made between the magnitude of a wheel load of a typical grain cart that could be applied to a field bridge and the magnitude of a wheel load applied in the experimental tests at ultimate load capacity of the bridge specimen. To qualify the comparative results, the load distribution relationship (based on the Timber Bridge Design Manual [2]) of a wheel load carried by a given stringer in a field bridge is used. The load distribution factor (i.e., the fraction of an applied wheel load carried by an individual stringer in a bridge) is defined as:

$$DF = \frac{S}{4} \text{ (for a single lane bridge)}$$

where,

DF = distribution factor

S = stringer spacing (ft.)

For a stringer spacing of 16 in. as in the experimental bridge specimens:

$$DF = \frac{1.33}{4} = 0.33 \text{ (wheels per stringer)}$$

Therefore, it would be assumed that a wheel load is carried equally by three stringers. Although, the design specification recommends the distribution of a wheel load to three stringers, in reality this is a conservative value, and near ultimate load conditions, more stringers would share in carrying the load. Therefore, the three stringer experimental bridge specimens (Bridges 3 and 4) represent more conservative results than for the five stringer bridge specimens (Bridges 1 and 2) relative to expected field bridge behavior.

Table 2 shows a wheel load summary of the experimental test results compared to an 875 bushel grain cart. An 875 bushel grain cart has a published axle load of approximately 57,000 lbs. (253.6 kN). Twenty percent, or 11,400 lbs (50.7 kN) is assumed to be transferred to the tow vehicle resulting in an actual cart axle load of 35,600 lbs. (158.4 kN). This is equivalent to a wheel load of 17,800 lbs. (79.2 kN). As noted in all four cases in the table, the experimental ultimate wheel load exceeded the wheel load of this particular cart.

Summary and Conclusions

Tests to failure were performed on four simple span stringer timber bridge sections. Two of the bridges consisted of five stringers and the other two had three stringers. Applied load, stringer mid-span deflections, photos, and videos were taken for each test, along with written and recorded notes. Load/deflection plots were developed and a description of the bridges behavior discussed. Comparisons were made between an expected wheel load for an 875 bushel, single axle grain cart and the wheel load measured in the experimental tests at ultimate loading.

Based on all four tests, there appears to be good load sharing between the stringers. The bridge failures could all be characterized as sudden and were due to flexural failures of the bridge stringers. No structural distress was noted in the deck panels, and no crushing of the sill plate under the stringers was noted. The bridge failure loads for Bridge 1 and Bridge 2 (containing five stringers) were 42,200 lbs. (187.7 kN) and 40,100 lbs. (178.4 kN), respectively. For Bridge 3 and Bridge 4 (containing three stringers), the failure loads were 27,200 lbs. (121.0 kN) and 36,300 lbs.

(161.5 kN), respectively. These loads exceed the wheel load that would be applied by an 875 bushel single axle grain cart.

REFERENCES

1. Mannering, F.L., W.P. Kilareski. "Principles of Highway Engineering and Traffic Analysis", Textbook, John Wiley & Sons, Inc., N.Y., New York, 1990.
2. Ritter, Michael A. "Timber Bridges: Design, Construction, Inspection, and Maintenance", United States Department of Agriculture, Forest Service, Engineering Staff, EM 7700-8, Washington, DC, June 1990

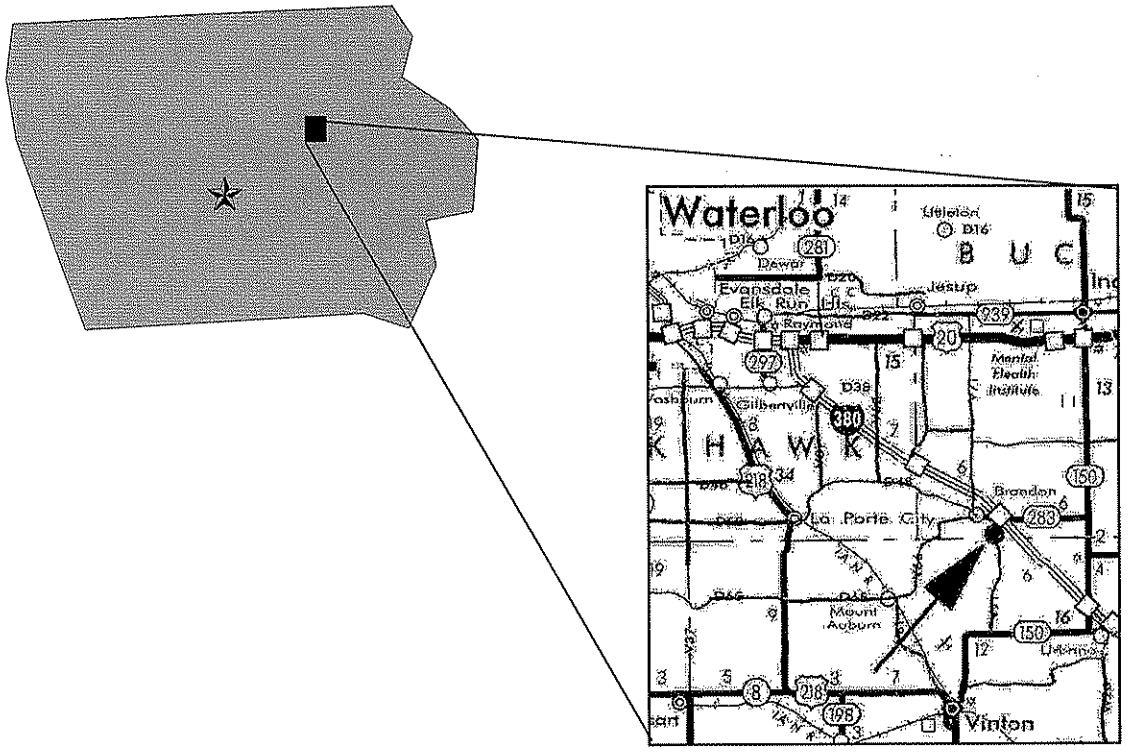

Figure 1. Location of PCC pavement test panel in Buchanan Co., Iowa.

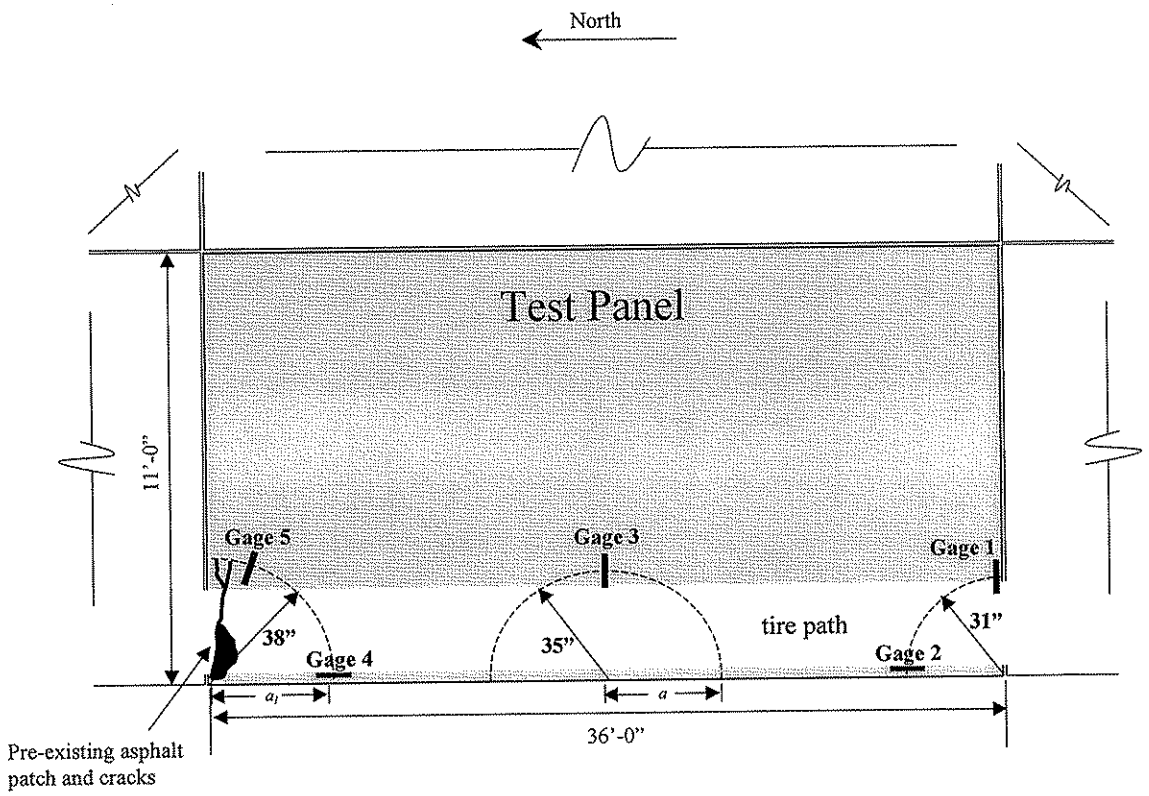

Figure 2. Strain gage layout and loading path on PCC pavement panel.

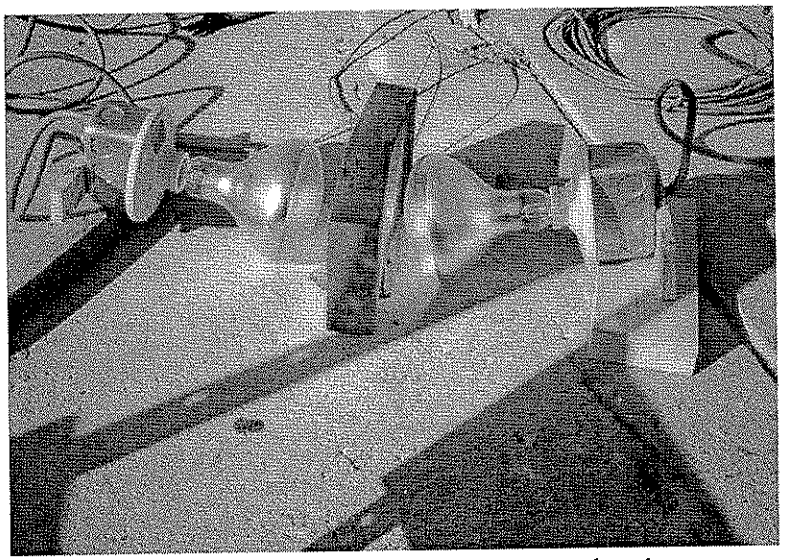

Figure 3. Curing of concrete surface mounted stain gage used on PCC pavement tests.

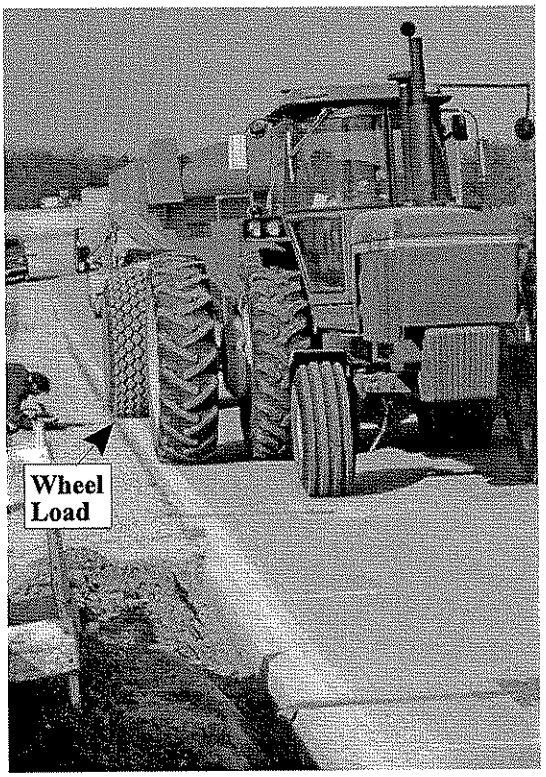

Figure 4. Tractor and grain cart test vehicle used on PCC pavement tests (looking north).

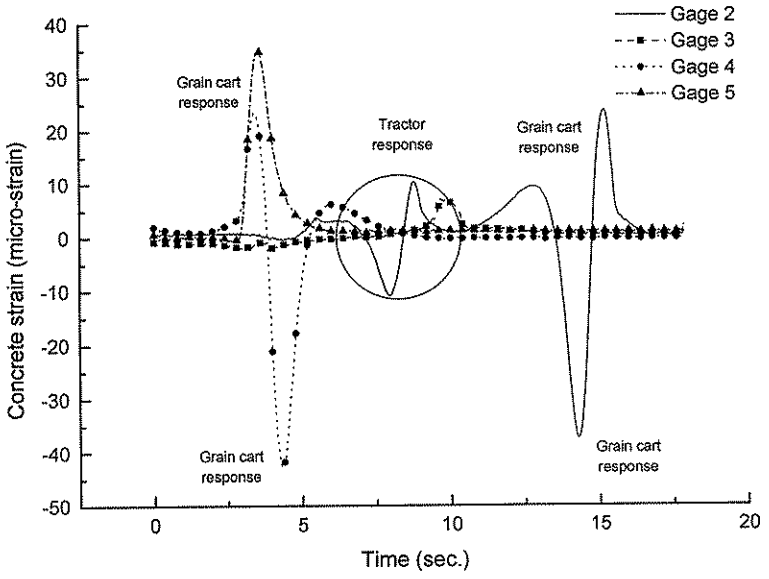

Figure 5. Test 12 strain vs. time plot with cart traveling north to south (left to right)

Table 1. Recorded pavement test strains.

Test	GAGE 2			GAGE 3			GAGE 4			GAGE 5		
	Max.	Min.	Max. Range	Max.	Min.	Max. Range	Max.	Min.	Max. Range	Max.	Min.	Max. Range
1	25	-42	67	9	-5	14	20	-35	55	200	-6	206
2	21	-26	47	5	-5	10	23	-46	69	68	-5	73
3	24	-43	67	49	-5	54	19	-34	53	125	-5	130
4	26	-32	58	-2	-16	14	24	-43	67	53	-6	59
5	23	-36	59	7	-4	11	21	-35	56	83	-3	86
6	24	-45	69	26	-9	35	25	-51	76	43	-5	48
7	22	-33	55	8	-5	13	24	-42	66	41	-4	45
8	22	-31	53	2	-9	11	20	-30	50	43	-12	55
9	17	-17	34	21	-6	27	18	-32	50	19	-13	32
10	26	-46	72	11	-5	16	25	-44	69	40	-2	42
11	24	-35	59	24	-4	28	20	-71	91	42	-9	51
12	25	-38	63	11	-4	15	25	-45	70	39	-3	42
13	28	-38	66	2	-19	21	26	-50	76	43	-5	48
14	22	-33	55	3	-5	8	22	-32	54	39	-4	43
15	27	-40	67	20	-2	22	24	-48	72	49	-5	54
16	21	-27	48	2	-9	11	20	-30	50	33	-5	38
17	24	-31	55	6	-4	10	15	-24	39	131	-19	150
18	27	-43	70	12	-4	16	23	-38	61	58	-4	62
19	21	-20	41	2	-32	34	27	-44	71	42	-5	47
20	28	-52	80	15	-3	18	26	-45	71	37	-10	47
21	25	-31	56	8	-7	15	27	-54	81	47	-4	51
22	31	-60	91	24	-7	31	29	-55	84	46	0	46
23	12	-14	26	27	-2	29	27	-62	89	46	-4	50
24	32	-65	97	20	-12	32	29	-59	88	47	-1	48
25	25	-32	57	-	-	-	33	-47	80	54	-4	58
26	33	-64	97	16	-23	39	29	-60	89	37	-9	46
27	26	-42	68	45	-11	56	17	-24	41	258	-12	270
28	31	-62	93	46	-7	53	28	-62	90	42	-5	47
AVG	25	-39	63	16	-8	24	24	-44	68	64	-6	71
MEDIAN	25	-37	61	11	-5	18	24	-44.5	69.5	44.5	-5	49

Note: + strains represent tension
- strains represent compression

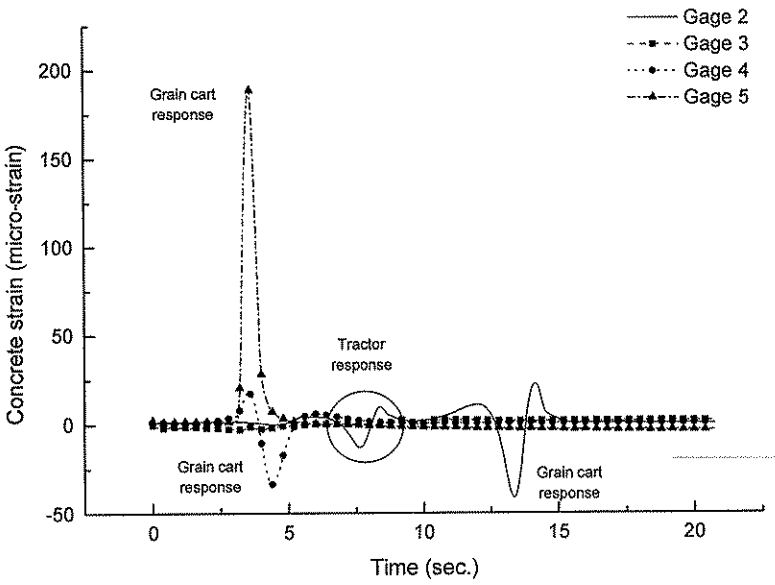

Figure 6. Test 1 strain vs. time plot with cart traveling north to south (left to right)

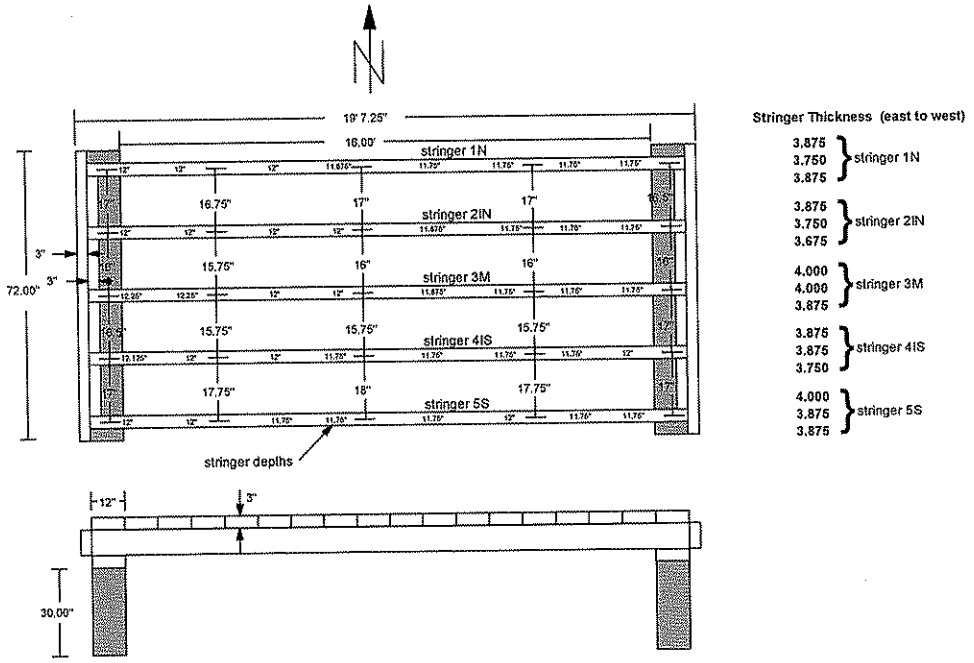

Figure 7. Measured dimensions for Bridge 1.

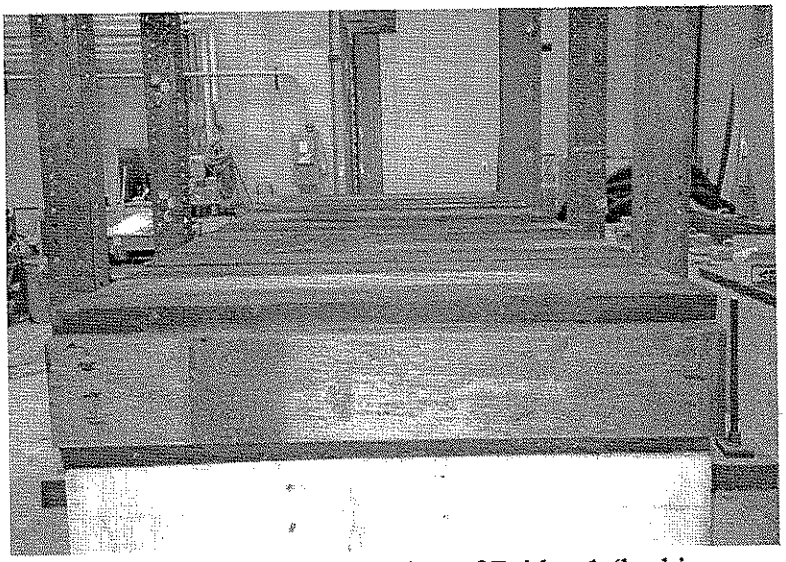

Figure 8. Completed construction of Bridge 1 (looking east).

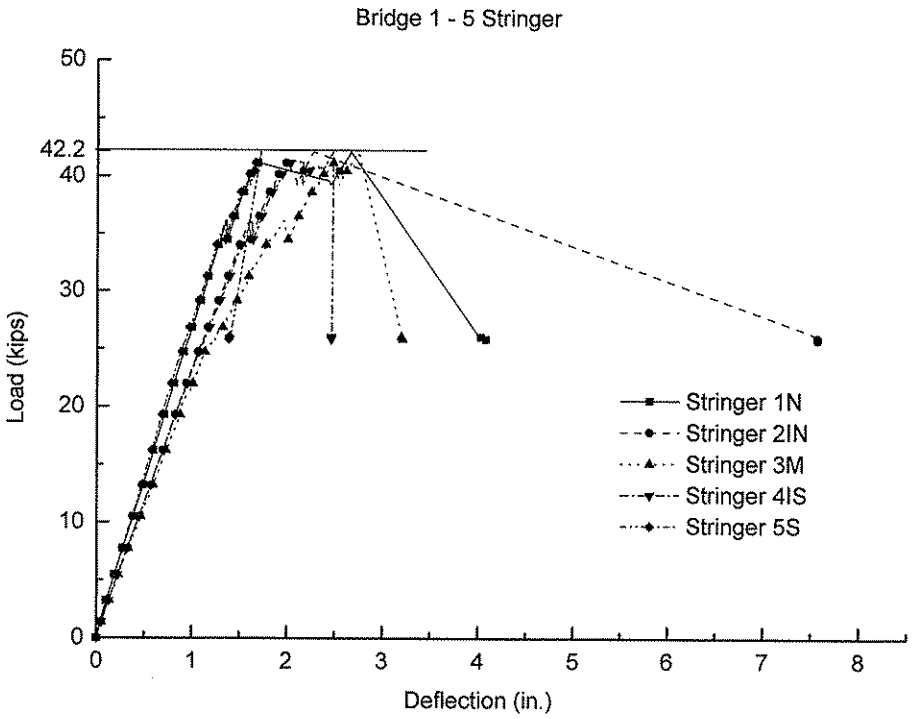

Figure 9. Load/deflection plot of Bridge 1.

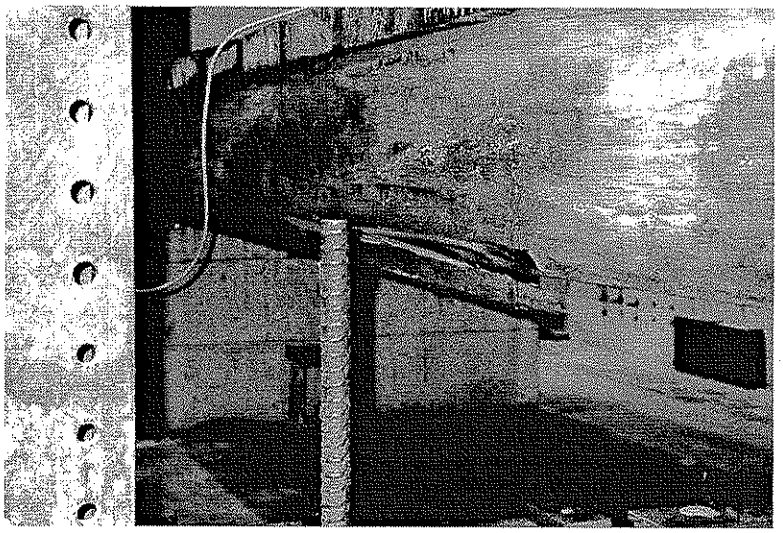

Figure 10. Stringer 1N failure - Bridge 1.

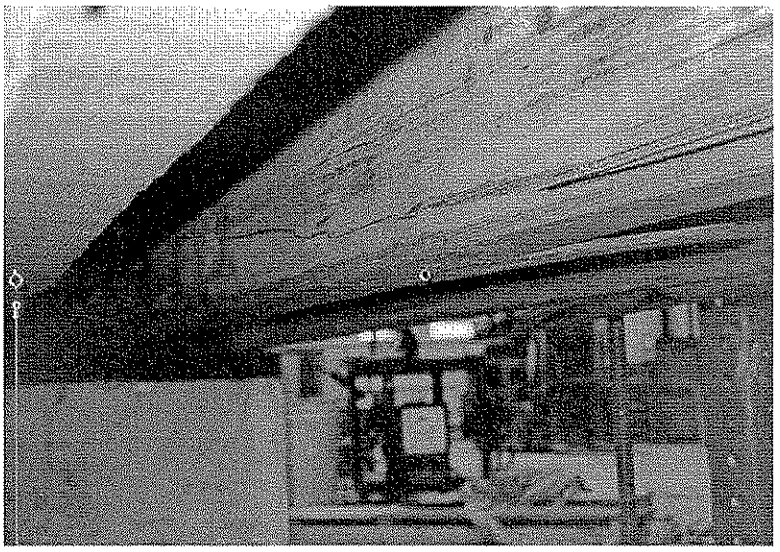

Figure 11. Stringer 2IN failure - Bridge 1.

Figure 12. Stringer 3M failure - Bridge 1.

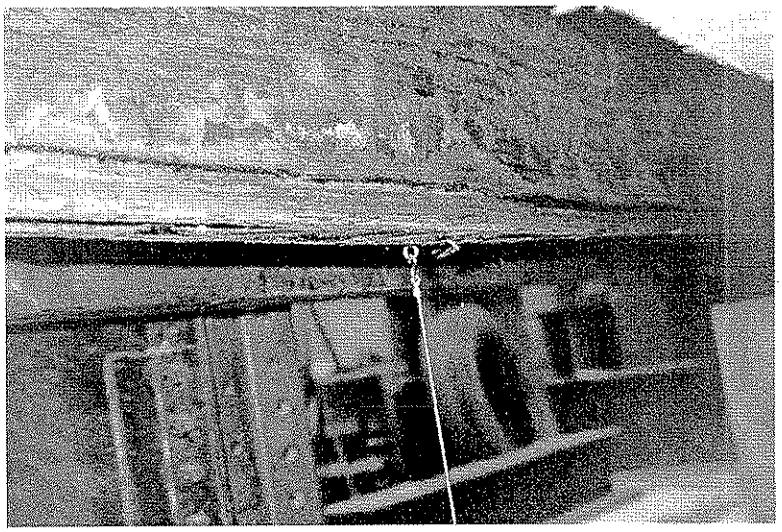

Figure 13. Stringer 4IS failure - Bridge 1.

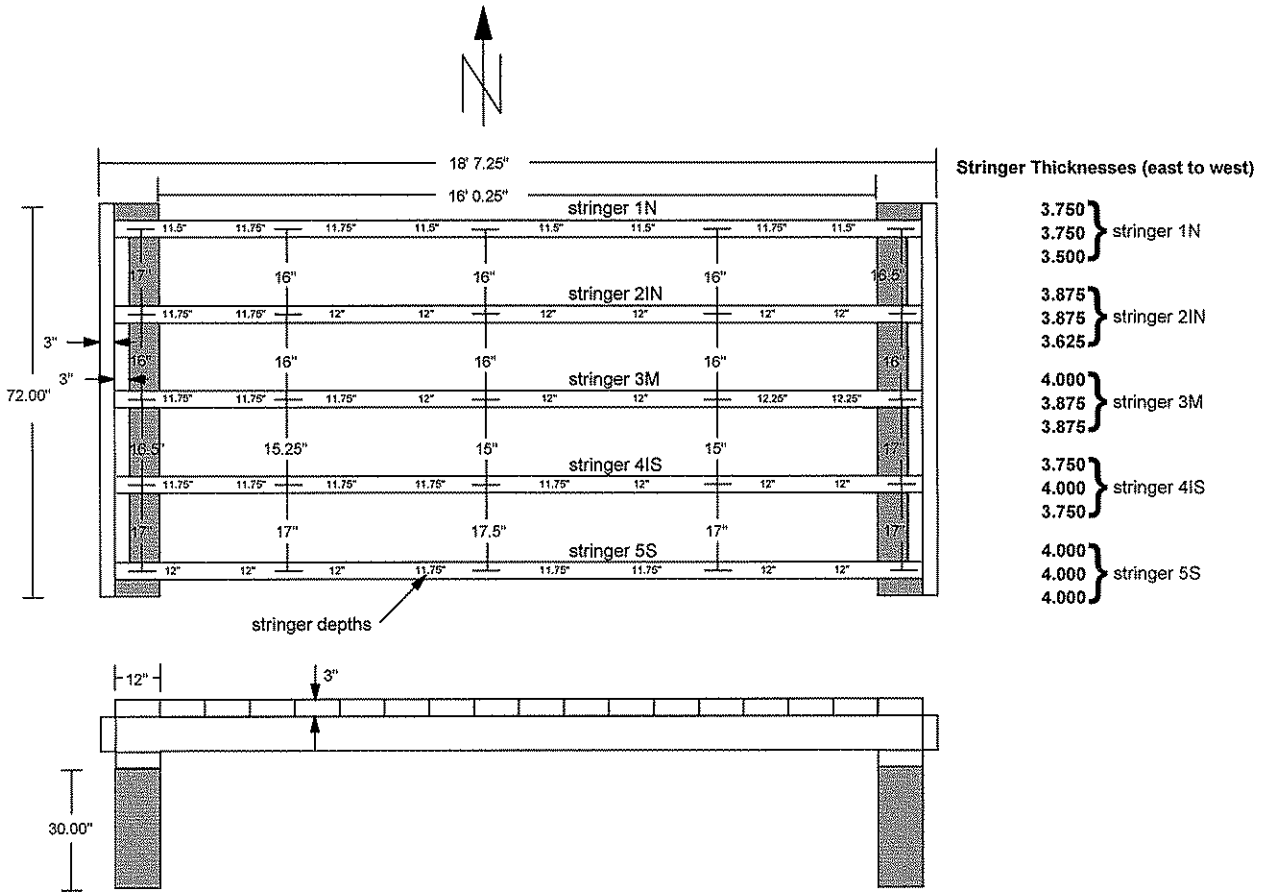

Figure 14. Measured dimensions for Bridge 2.

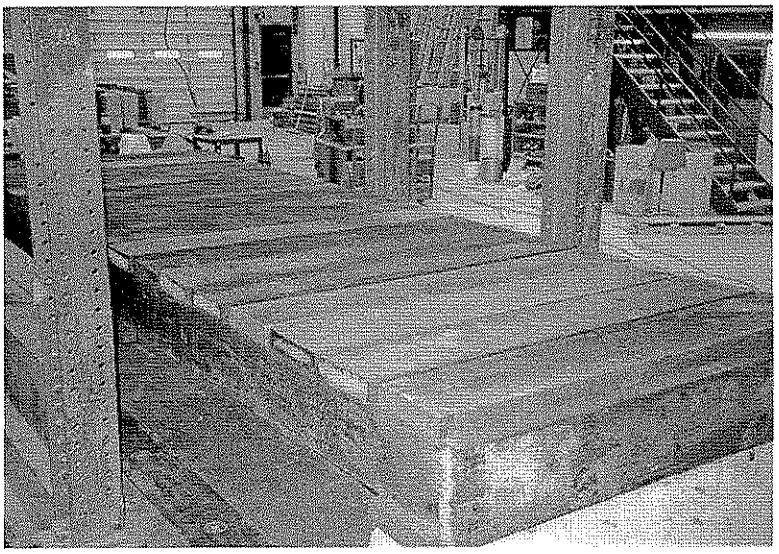

Figure 15. Completed construction of Bridge 2.

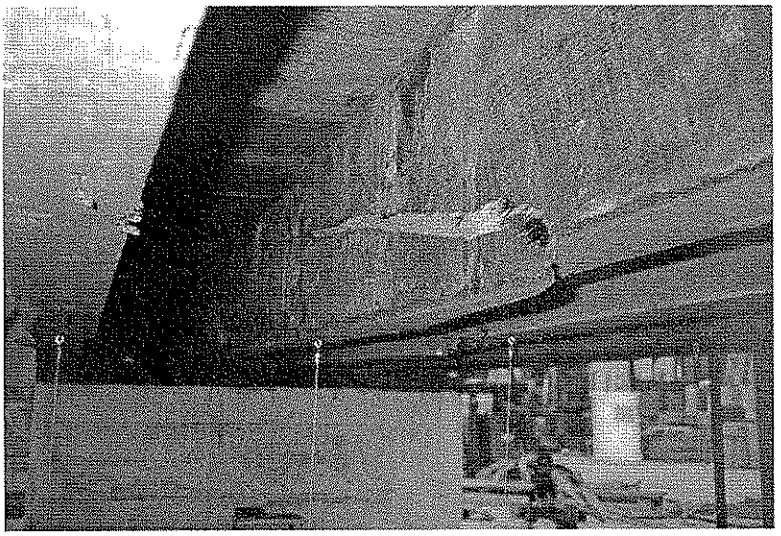

Figure 16. Stringer 4IS failure initiated in the vicinity of a knot - Bridge 2.

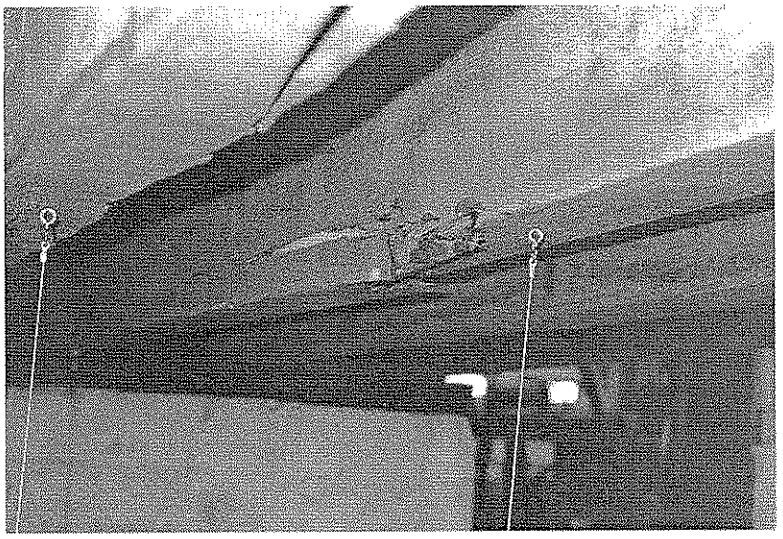

Figure 17. Stringer 3M failure at knot location in tension face - Bridge 2.

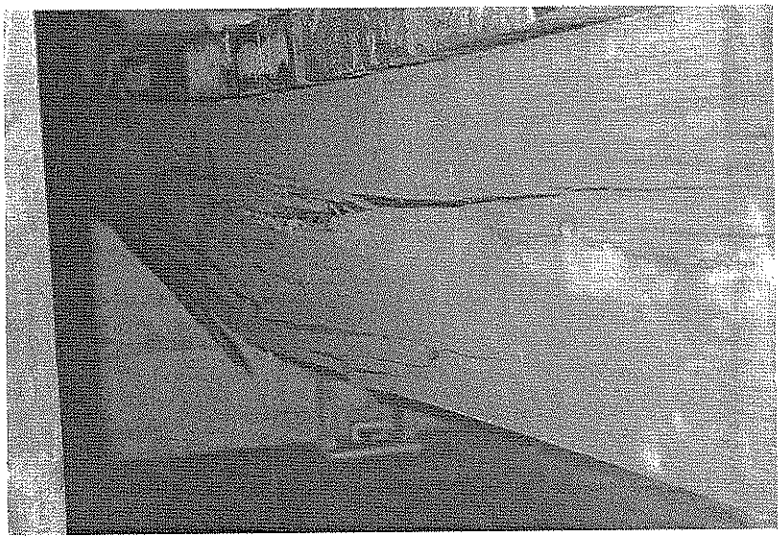

Figure 18. Stringer 5S failure - Bridge 2.

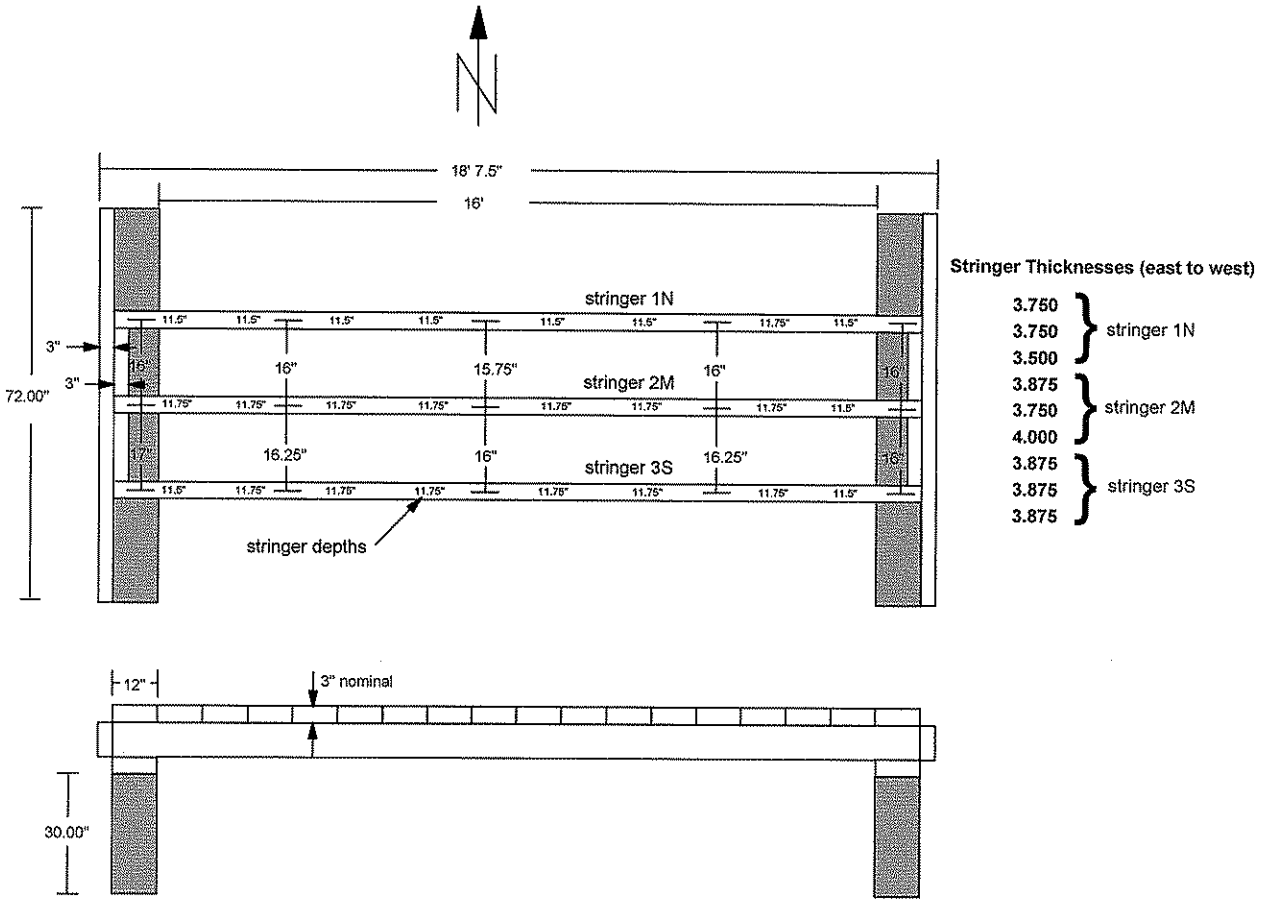

Figure 19. Measured dimensions for Bridge 3.

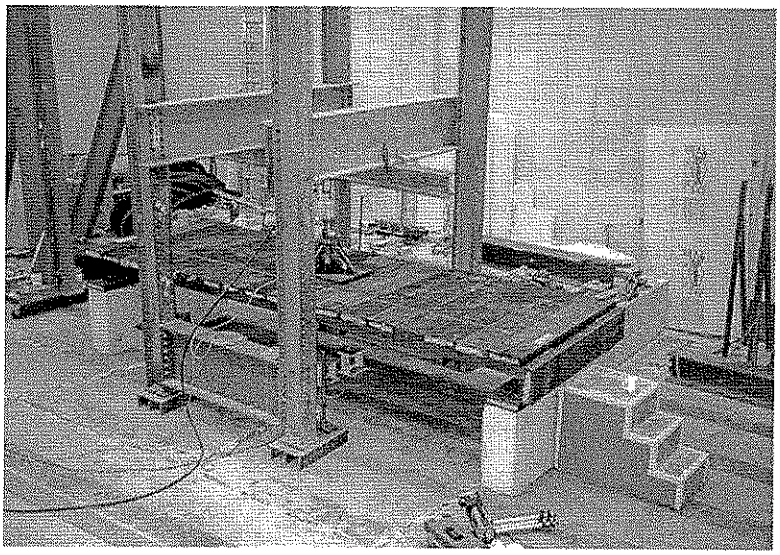

Figure 20. Bridge 3 prior to testing.

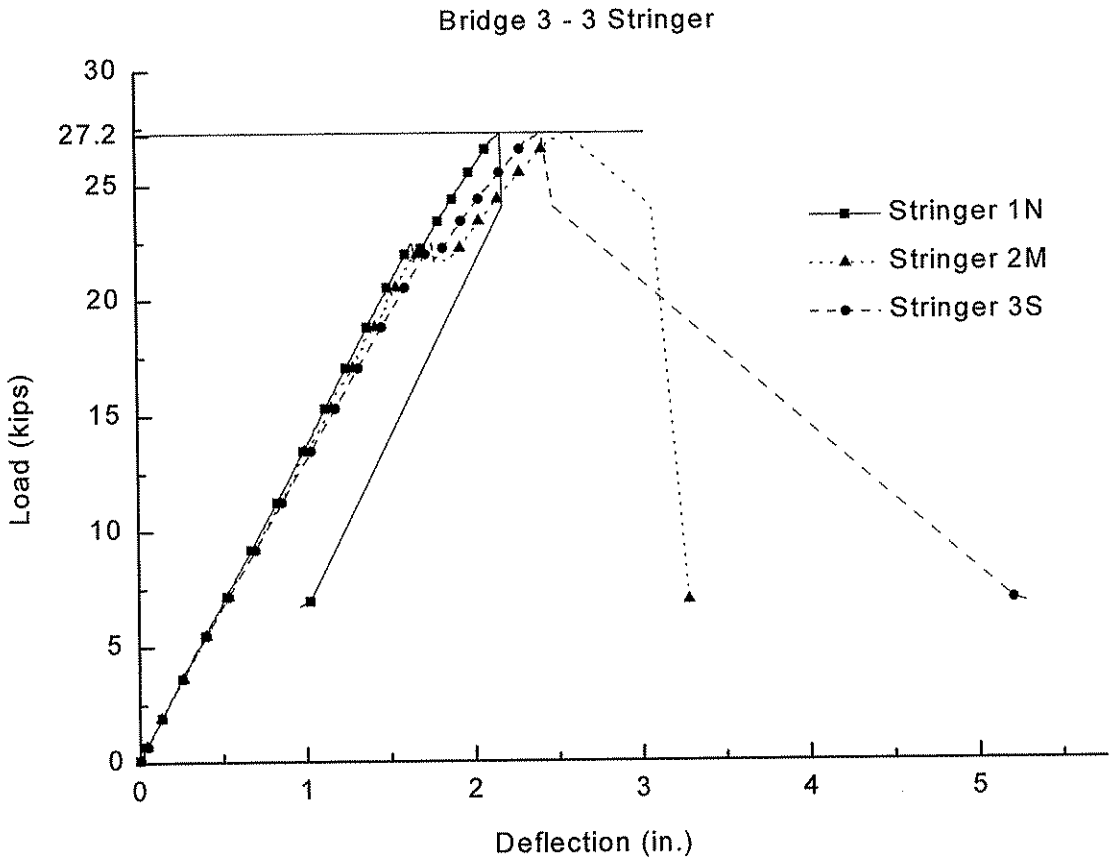

Figure 21. Load/deflection plot of Bridge 3.

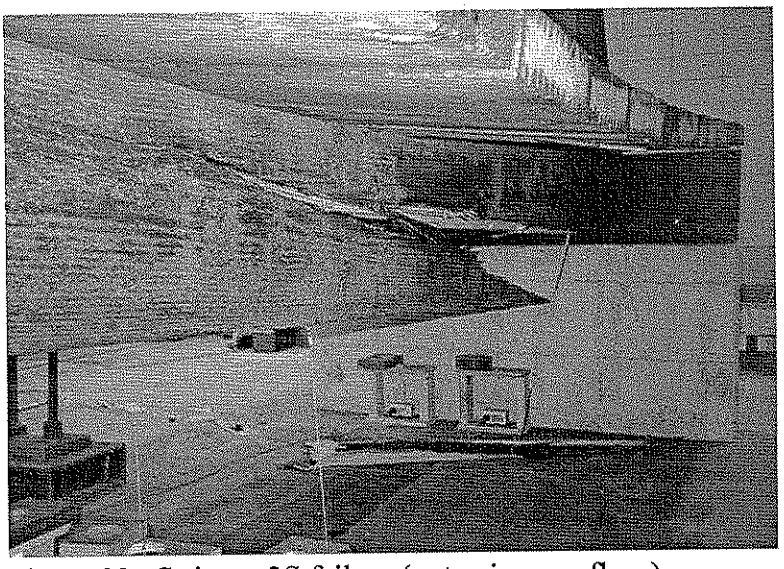

Figure 22. Stringer 3S failure (note piece on floor) - Bridge 3.

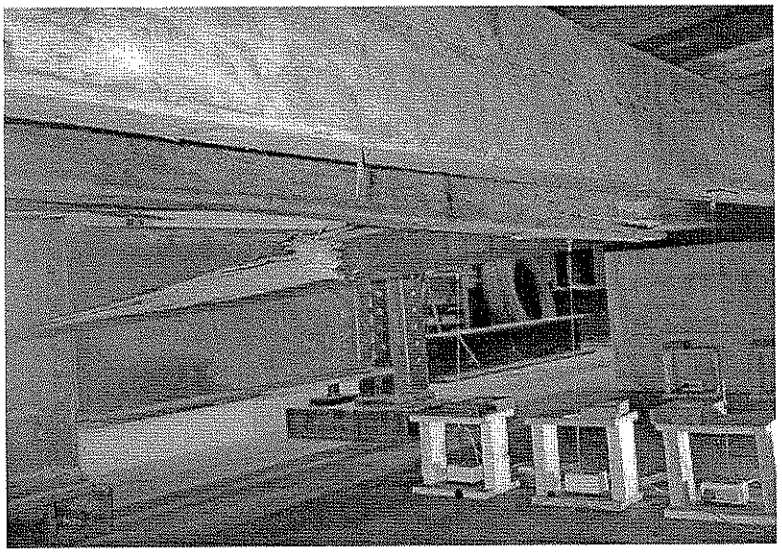

Figure 23. Stringers 1N, 2M and 3S (from right to left) after bridge failure - Bridge 3.

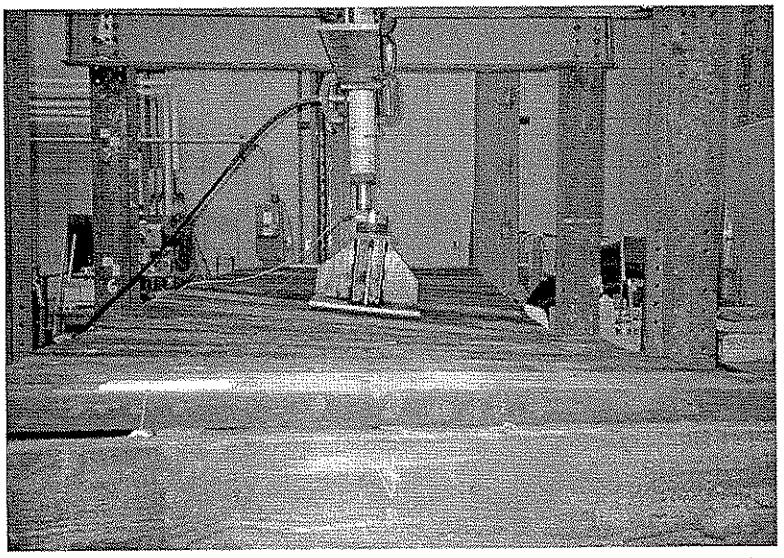

Figure 24. Bridge 3 after failure of stringers (looking east).

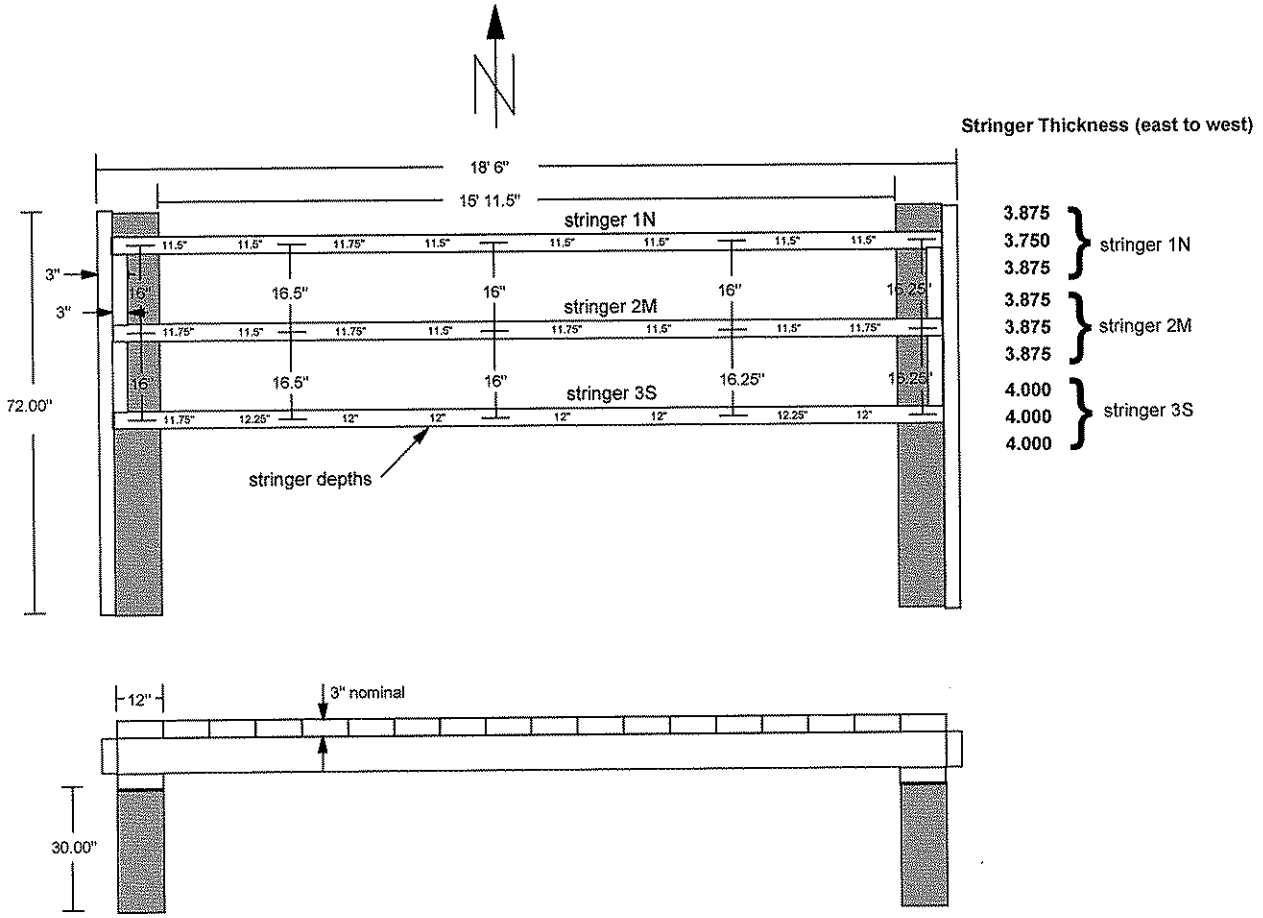

Figure 25. Measured dimensions for Bridge 4.

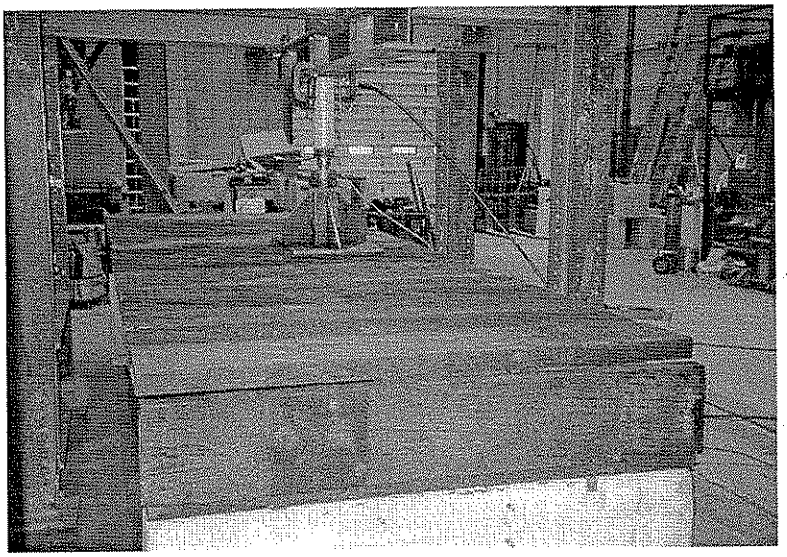

Figure 26. Bridge 4 prior to testing (looking west).

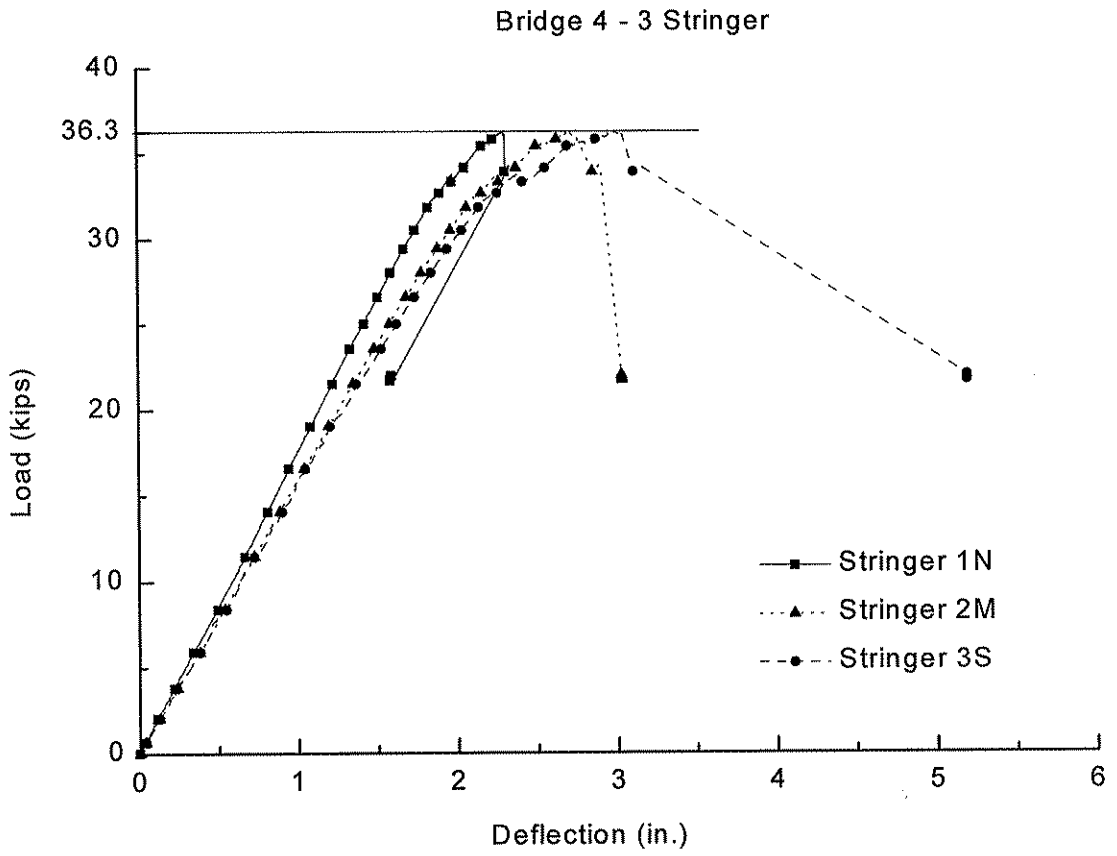

Figure 27. Load/deflection plot of Bridge 4.

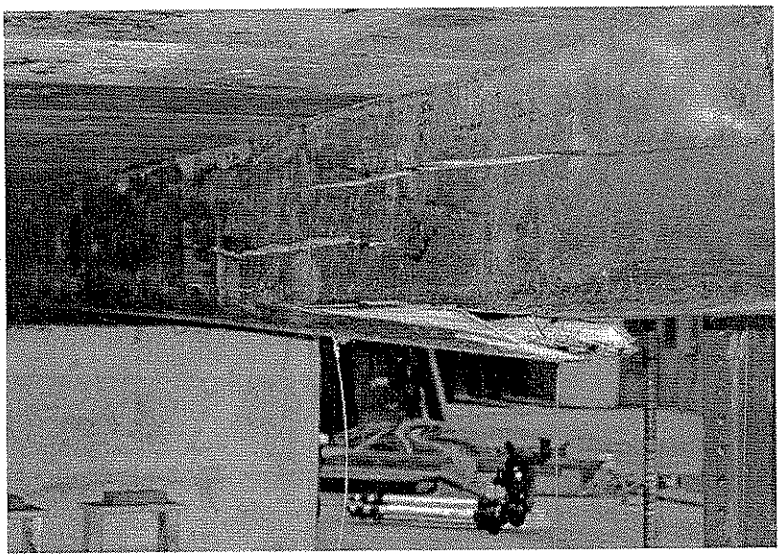

Figure 28. Stringer 3S failure - Bridge 4.

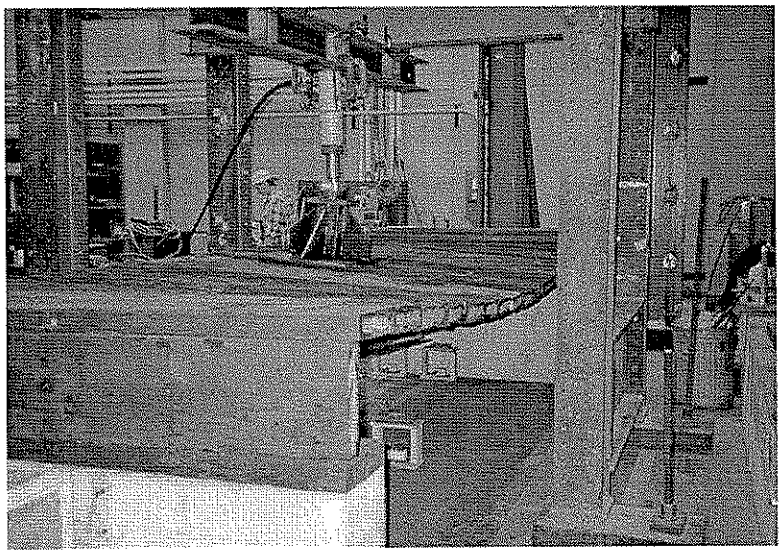

Figure 29. Bridge 4 after failure of stringers (looking east).

Table 2. Wheel load comparisons of experimental test results with 875 bushel, single axle, grain cart.

Test	# of Stringers	Grain Cart Wheel Load lbs. (kN)	Experimental Ultimate Wheel Load lbs. (kN)	Ratio of Experimental Load to Grain Cart Load
Bridge 1	5	17,800 (79.2)	42,200 (187.7)	2.37
Bridge 2	5	17,800 (79.2)	40,100 (174.4)	2.25
Bridge 3	3	17,800 (79.2)	27,200 (121.0)	1.53
Bridge 4	3	17,800 (79.2)	36,300 (161.5)	2.04